View Article Online
View Journal

Green Chemistry

Cutting-edge research for a greener sustainable future

Accepted Manuscript

This article can be cited before page numbers have been issued, to do this please use: A. khazaee, R. Jahanshahi, S. Sobhani, J. Skibsted and J. Sansano, *Green Chem.*, 2020, DOI: 10.1039/D0GC01274B.

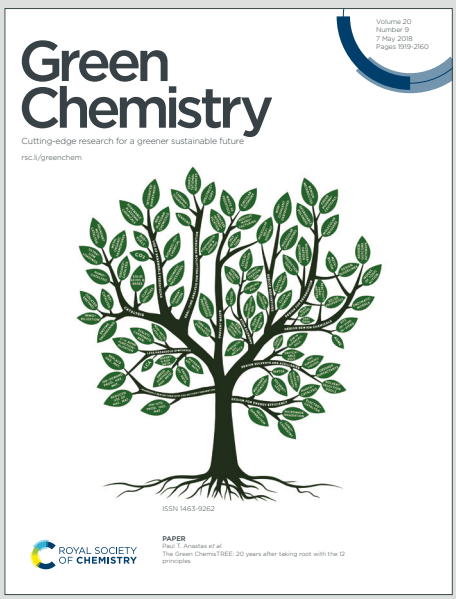

This is an Accepted Manuscript, which has been through the Royal Society of Chemistry peer review process and has been accepted for publication.

Accepted Manuscripts are published online shortly after acceptance, before technical editing, formatting and proof reading. Using this free service, authors can make their results available to the community, in citable form, before we publish the edited article. We will replace this Accepted Manuscript with the edited and formatted Advance Article as soon as it is available.

You can find more information about Accepted Manuscripts in the Information for Authors.

Please note that technical editing may introduce minor changes to the text and/or graphics, which may alter content. The journal's standard Terms & Conditions and the Ethical guidelines still apply. In no event shall the Royal Society of Chemistry be held responsible for any errors or omissions in this Accepted Manuscript or any consequences arising from the use of any information it contains.

View Article Online
DOI: 10.1039/D0GC01274B

ARTICLE

Immobilized piperazine on the surface of graphene oxide as a heterogeneous bifunctional acid-base catalyst for the multicomponent synthesis of 2-amino-3-cyano-4*H*-chromenes

Received 00th January 20xx,
Accepted 00th January 20xx

DOI: 10.1039/x0xx00000x

Asma Khazaee,[a] Roya Jahanshahi,[a] Sara Sobhani,*[a] Jørgen Skibsted [b] and José Miguel Sansano[c]

The immobilized piperazine on the surface of graphene oxide (piperazine-GO) is synthesized and characterized by different methods such as FT-IR, solid-state $^{29}Si\{^{1}H\}$ and $^{13}C\{^{1}H\}$ CP/MAS NMR, elemental analysis, TGA, TEM, FE-SEM, XPS, and TPD. Subsequently, it is used as a heterogeneous bifunctional acid-base catalyst for the efficient multicomponent reaction of malononitrile, different active compounds containing enolizable C–H bonds and various aryl/alkyl aldehydes in aqueous ethanol. A wide variety of 2-amino-3-cyano-4*H*-chromenes are synthesized in the presence of this heterogeneous catalyst in good to high yields and with short reaction times. The catalyst is easily separated and reused for at least six times without significant loss of activity. The acidic nature of GO improves the catalytic activity of the supported piperazine and also provided heterogeneity to the catalyst. Using aqueous ethanol as a green solvent, high turnover numbers (TON), facile catalyst recovery and reuse, simple work-up and generality of the method, make this protocol an environmentally benign procedure for the synthesis of the titled heterocycles.

Introduction

Multicomponent reactions (MCRs), which eliminate the isolation of intermediates and reduce the number of discrete chemical steps, waste products and operational costs, have been acknowledged as essential tools for the green synthesis of organic compounds.[1-3] These kinds of reactions allow a rapid and efficient synthesis of complex molecules from simple starting materials. Most routes followed in MCRs are nucleophilic reactions. An ideal pathway for nucleophilic reactions is dual activation of both the electrophiles and nucleophiles by acidic and basic catalysts, respectively.[4-10] Obviously, the use of both homogeneously strong acidic and basic species in a single reactor is impossible due to the neutralization that forms inactive salts. Moreover, the recovery and reuse of both acidic and basic catalysts are industrially problematic and result in product contamination. To solve this problem, the concept of 'site isolation', which is inspired by enzymatic catalysis, has been followed. A well understood fact in biochemistry is that the presence of spatially separated incompatible sites on the enzymes avoids undesired interactions. This implies that the enzymes are capable of accelerating reactions through cooperative interactions between accurately positioned functional groups present in their active sites.[11-13] Mimicking enzymatic catalysis, significant progress has recently been achieved in the synthesis of bifunctional catalysts by immobilization of mutually incompatible catalysts such as acids and bases on different solid materials such as silica, SBA-15, MCM-41, clays, polymers, etc.[14-23] Furthermore, these heterogeneous catalysts can be recovered and reused, making the entire process greener. However, there are several evident barriers in the preparation of these catalysts such as tedious protection–deprotection procedures or the uncontrollable and inhomogeneous positioning of catalytically active species.[24-27] Moreover, some of them exhibit unsatisfactory catalytic efficiencies due to the enhanced steric hindrance.[28,29] Therefore, the development of a simple and efficient method for the construction of heterogeneous bifunctional acid–base catalysts is strongly needed.

Recently, graphene oxide (GO) with significant mechanical strength and remarkable thermal stability has received increasing interest as carbocatalyst and catalyst support owing to its unique structural and surface properties.[30-33] GO with a two-dimensional sheet-like structure has a high surface area that is readily accessible to the reactants with negligible mass transfer resistance, which is distinct from conventional porous materials. The presence of several oxygen containing functionalities, such as epoxide and hydroxyl groups on the surface of GO sheets provides its facile functionalization by different functional groups.[34-37] Moreover, GO has intrinsic acidic properties due to the presence of carboxylic acids along the sheet edges. Taking advantage of the presence of intrinsic carboxylic acids on GO, bifunctional acid-base GO catalysts have been synthesized by a simple post grafting of basic functional groups onto GO.[38-40] The synthesized bifunctional acid-base GO catalysts exhibited an excellent synergic effect by the grafted basic groups on the plane of GO and the adjacent intrinsic carboxylic acids along the edges. Furthermore, they could be easily recycled and reused repetitively. However, despite the excellent catalytic activity and reusability of bifunctional GO catalysts, only a few studies focused on the GO functionalization and its use as bifunctional GO catalysts in MCRs, even though this area has an immense potential.[35,41-46]

[a] Address: Department of Chemistry, College of Sciences, University of Birjand, Birjand, Iran, email: ssobhani@birjand.ac.ir, sobhanisara@yahoo.com.
[b] Department of Chemistry and Interdisciplinary Nanoscience Center (iNANO), Aarhus University, Langelandsgade 140, DK-8000, Aarhus C, Denmark.
[c] Departamento de Química Orgánica, Facultad de Ciencias, Centro de Innovación en Química Avanzada (ORFEO-CINQA) and Instituto de Síntesis Orgánica (ISO), Universidad de Alicante, Apdo. 99, 03080-Alicante, Spain.

Within heterocyclic compounds, 2-amino-3-cyano-4*H*-chromenes and their derivatives have attracted significant interest, because they are present in a wide variety of biologically active natural products and exhibit several pharmaceutical properties such as anti-allergic, anti-oxidant and antibacterial.[47-50] These compounds have also been known as spasmolytic, anti-malaria, diuretic, anti-cancer, anti-HIV, anti-Alzheimer, anti-coagulant, and anti-anaphylactic agents.[51,52] Figure 1 shows some bioactive chromene derivatives. Thus, the preparation of these heterocyclic cores has extended a high reputation in heterocyclic chemistry. Several strategies have been reported for the synthesis of 2-amino-3-cyano-4*H*-chromenes, mostly *via* a three-component reaction involving the cyclo-condensation of differently substituted aldehydes, various β-dicarbonyl compounds, and alkyl malonates.[53-58] Although the reported protocols find certain merits of their own, still they suffer from a number of demerits such as relying on the tedious work-up procedure, use of hazardous and/or costly catalysts and volatile organic solvents, high reaction times, low yields and lack of generality for the synthesis of 2-amino-3-cyano-4*H*-chromenes starting from aliphatic aldehydes. More importantly, in spite of the prominence of bifunctional catalysts for the efficient promotion of MCRs, systematic investigations of bifunctional catalysts for the three-component synthesis of 2-amino-3-cyano-4*H*-chromenes are rare in the literature.[35,59-68] Therefore, the introduction of a simple and green procedure for the multicomponent synthesis of 2-amino-3-cyano-4*H*-chromenes, catalyzed by an efficient, inexpensive and reusable bifunctional catalyst, is a valid goal in the synthesis of chromenes, considering the growing importance of bifunctional catalysts in organic synthesis.

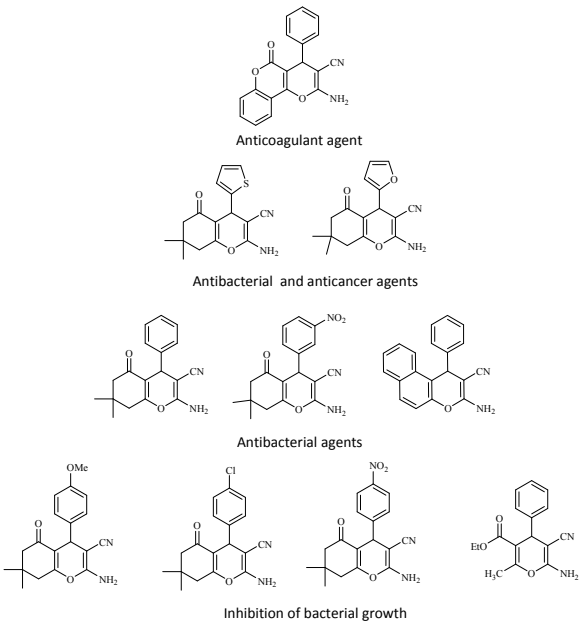

Figure 1. Pharmacologically active 2-amino-3-cyano-4*H*-chromenes

To benefit the valuable applications of multifunctional catalysts in MCRs, and as a part of our research program to develop efficient and green methods in organic synthesis,[69-74] herein we report the synthesis of immobilized piperazine on the surface of graphene oxide as a new heterogeneous catalyst. This catalyst is characterized by different methods including FT-IR, solid-state $^{29}Si\{^1H\}$ and $^{13}C\{^1H\}$ CP/MAS NMR, elemental analysis, TGA, TEM, FE-SEM, XPS and TPD. We also demonstrate its applicability as a reusable bifunctional acid-base catalyst for the three-component condensation reaction of various β-dicarbonyl compounds, malononitrile and aryl/alkyl/heteroaryl aldehydes.

Experimental

All chemicals were purchased from Merck Chemical Company. Liquid-state ^1H NMR spectra were recorded on a Bruker Advance DPX-300 spectrometer, using $CDCl_3$ and DMSO solvents and TMS as the internal standard. The purity of the products and the progress of the reactions were accomplished by TLC on silica-gel polygram SILG/UV254 plates. FT-IR spectra were recorded on a Shimadzu Fourier Transform Infrared Spectrophotometer (FT-IR-8300). Solid-state $^{13}C\{^1H\}$ and $^{29}Si\{^1H\}$ CP/MAS NMR spectra were obtained on a Bruker Avance II 400 MHz spectrometer (9.39 T) and a Varian INOVA 300 MHz spectrometer (7.05 T) using 4 mm and 5 mm CP/MAS NMR probes, respectively. The $^{13}C\{^1H\}$ CP/MAS spectra employed a 10.0 kHz spinning speed, a CP-contact time of 1.0 ms, a 4-s relaxation delay, and 16384 scans. The $^{29}Si\{^1H\}$ CP/MAS NMR spectrum was acquired with a 5.0 kHz spinning speed, a CP-contact time of 1.0 ms, a 4-s relaxation delay, and 20.000 scans. ^{13}C and ^{29}Si chemical shifts are relative to neat TMS. Elemental analysis was carried out on a Costech 4010 CHNS elemental analyzer. Thermogravimetric analysis (TGA) was performed using a Shimadzu thermogravimetric analyzer (TG-50) using a heating rate of 10 °C min^{-1} under atmospheric air. TEM analysis was performed with a TEM microscope (Philips CM30). Field emission scanning electron microscopy (FE-SEM) was obtained with a FE-SEM (model Mira 3-XMU). XPS analyses were performed using a VG-Microtech Multilab 3000 spectrometer, equipped with an Al anode. The deconvolution of the spectra was carried out using Gaussian–Lorentzian curves. NH_3 and CO_2 temperature-programmed desorption (NH_3-TPD and CO_2-TPD) experiments were carried out using a NanoSORD NS91 apparatus (Sensiran Co., Iran). The NH_3-TPD experiment was performed on 50 mg of the catalyst placed in a U-shaped quartz reactor. Prior to the TPD run, the catalyst was degassed in a flow of 10 cm^3/min He at 400 °C for 1 h and then cooled down to 110 °C. This was followed by the adsorption of 5% NH_3/He at 110 °C for 30 min. The sample was then purged in a He stream for 30 min at 110 °C in order to remove loosely bound ammonia. Then, the sample was heated again from 110 to 750 °C at a heating rate of 10 °C/min in a flow of He (10 cm^3/min). The CO_2-TPD experiment was performed on 50 mg of catalyst placed in a U-shaped quartz reactor. Prior to the TPD run, the catalyst was degassed in a flow of 10 cm^3/min He at 400 °C for 1 h, and cooled down to 25 °C. This was followed by the adsorption of 20% CO_2/He at 25 °C for 30 min. Sample was then purged in a He stream for 60 min at 25 °C in order to remove loosely bound CO_2. Then, the sample was heated again from 25 to 800 °C at a heating rate of 10 °C/min in a flow of He (10 cm^3/min).

Synthesis of chloro-functionalized GO

A mixture of GO[41] (1 g) in toluene (50 mL) was sonicated for 30 min. 3-Chloropropyl trimethoxysilane (1.8 mL) was added to the dispersed GO in toluene (50 mL), slowly heated to 110 °C and stirred at this temperature for 20 h. Then, the reaction was cooled to room temperature. The resulting chloro-functionalized GO was centrifuged, washed three times with H_2O and ethanol, and dried at 80 °C in an oven under vacuum.

Synthesis of piperazine-GO

A mixture of chloro-functionalized GO (1 g) in toluene (20 mL) was sonicated for 30 min. Piperazine (0.43 g) was added to the dispersed chloro-functionalized GO (1 g) in dry toluene (20 mL), and the mixture was stirred for 6 h. The solid material was separated by centrifugation, washed with H_2O and ethanol, and dried at room temperature in vacuum to produce piperazine-GO.

General procedure for the synthesis of 2-amino-3-cyano-4*H*-chromenes in the presence of piperazine-GO

Aldehyde (1 mmol), dimedone (0.14 g, 1 mmol) and malononitrile (0.066 g, 1 mmol) were added to a mixture of piperazine-GO (0.004 g) in EtOH:H_2O (1:1, 1 mL). The reaction mixture was stirred at 50 ˚C and monitored by TLC untill no further progress in the reaction was observed. Then, the reaction mixture was cooled to room temperature. EtOH (5 mL) was added to the reaction mixture and the catalyst was separated by centrifugation, washed with EtOH (5 mL), dried and re-used for a consecutive run under the same reaction conditions. The solvent of the combined organic layer was evaporated under reduced pressure to obtain a residue, which was recrystallized in EtOH to produce the pure product.

Results and Discussion

Synthesis and characterization of piperazine-GO

Immobilized piperazine on the surface of graphene oxide (piperazine-GO) was synthesized following the procedure outlined in Scheme 1. At first, chloro-functionalized GO was synthesized by the reaction of GO with 3-chloropropyltrimethoxysilane in refluxing dry toluene. Subsequently, piperazine-GO was obtained by the reaction of chloro-functionalized GO with piperazine.

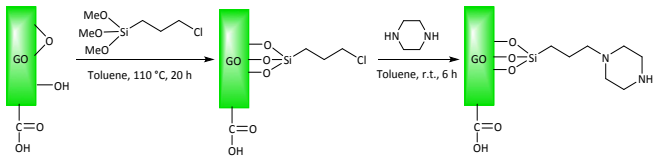

Scheme 1. Synthesis of piperazine-GO.

FT-IR spectra of GO and piperazine-GO are shown in Figure 2. The FT-IR spectrum of GO contains peaks with strong intensities at 1040, 1125, 1585, 1735, and 3438 cm^{-1}, which are attributed to the stretching vibrations of C-O-C, C-OH, C=C, C=O and O-H bonds, respectively. These peaks reveal the presence of hydroxyl, carboxyl, and epoxy groups on the GO. In the FT-IR spectrum of piperazine-GO, typical bands at about 2959 and 2857 cm^{-1} were assigned to the C-H stretching vibrations of alkyl chains. In this spectrum, Si-O-Si and Si-O-C stretching modes of silane chains appeared as a strong broad doublet at about 1100 and 1020 cm^{-1}. Importantly, in the FT-IR spectrum of piperazine-GO, the absorption band related to the C=O bonds of the carboxylic acids was observed at about 1725 cm^{-1}. In addition, the C–N stretching vibrations were positioned at about 1240 cm^{-1}.

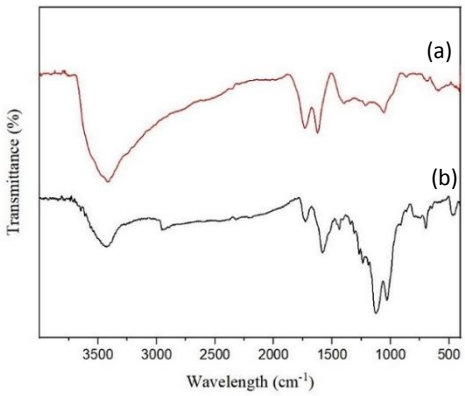

Figure 2. FT-IR spectra of (a) GO and (b) piperazine-GO.

The presence of the desired functional groups on the GO was qualitatively confirmed by solid-state magic-angle-spinning (MAS) NMR spectroscopy. The broadened resonance in the $^{29}Si\{^1H\}$ MAS NMR spectrum of piperazine-GO (Figure 3a), with the main intensity at -68.1 ppm, corresponds to T^3 [R–Si(O–C)$_3$] structural environments and thereby confirmes the successful incorporation of the organic silane moieties on the GO. Furthermore, the resonances at 8.4 (C_1), 24.8 (C_2) and 45.4 ppm (C_3 overlapped with C_4 and C_5) in the $^{13}C\{^1H\}$ CP/MAS NMR spectrum (Figure 3b) verify the structure of the supported piperazine on the surface of GO. The observed broadened peaks at 60, 72, 124 and 168 ppm are assigned to C-OH, epoxy (C-O-C), C=C and carboxyl groups, respectively.

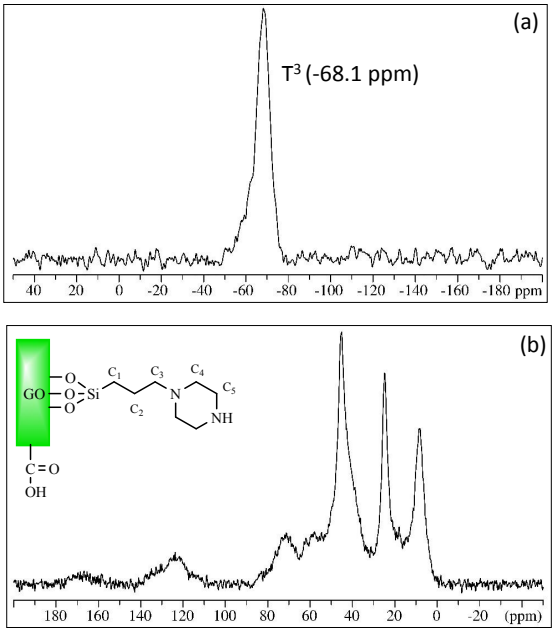

Figure 3. (a) $^{29}Si\{^{1}H\}$ CP/MAS NMR spectrum (7.05 T) of piperazine-GO obtained with a spinning speed of 5.0 kHz and a CP contact time of 1.0 ms. (b) $^{13}C\{^{1}H\}$ CP/MAS NMR spectrum (9.39 T) of piperazine-GO obtained with a spinning speed of 10.0 kHz and a CP contact time of 1.0 ms.

Elemental analysis showed that the loading of piperazine on the GO was 2.38 mmol.g^{-1} based on the nitrogen content (N = 6.69%).

The thermal stabilities of the piperazine-GO and GO were examined by TGA (Figure 4). As presented in Figure 4a, a total weight loss of about 55.4% was determined from the TGA curve of the piperazine-GO. A mass loss at below 135 °C, due to the loss of intercalated water molecules, and a weight loss from 135 to 195 °C, due to the decomposition of various oxygen functional groups, were also observed in the TGA curves of piperazine-GO and GO. The total mass loss of GO (Figure 4b) is obviously higher than that of piperazine-GO (Figure 4a), especially the second mass loss, which demonstrates the higher thermal stability of piperazine-GO owing to the logical decrease in the amount of oxygen-containing functional groups in the modified GO.[75-77] The final mass loss in the TGA curve of piperazine-GO (Figure 4a) is caused by the decomposition of organic parts located on its surface.

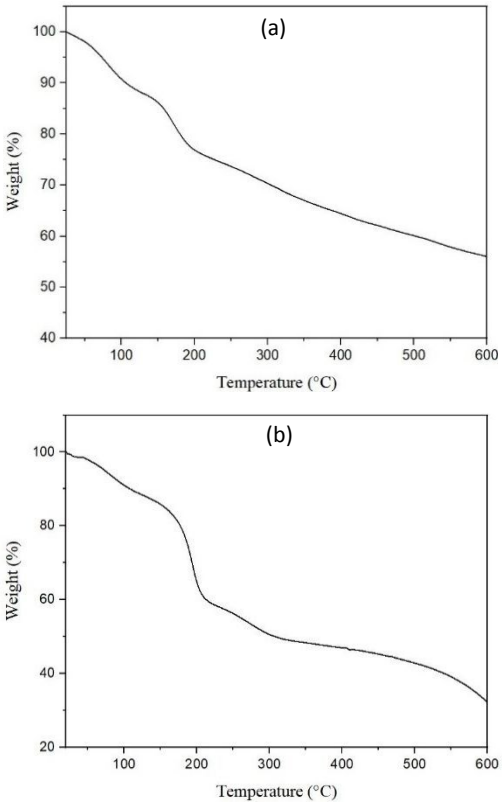

Figure 4. TGA curves for (a) piperazine-GO and (b) GO.

The morphological properties of piperazine-GO were examined by means of TEM and FE-SEM. The TEM and FE-SEM images of piperazine-GO (Figure 5) revealed the nanoscopic features of GO with a crumpling two-dimensional structure.

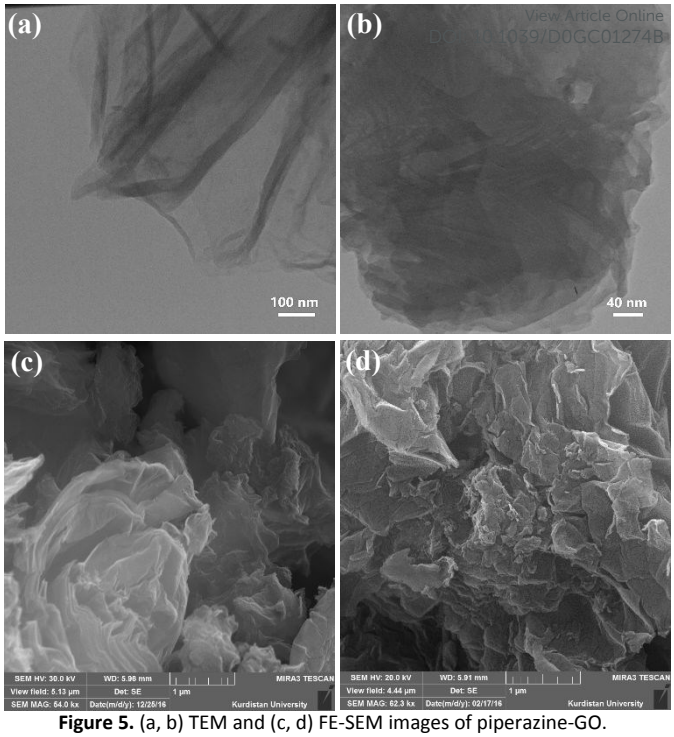

Figure 5. (a, b) TEM and (c, d) FE-SEM images of piperazine-GO.

The electronic properties of piperazine-GO were studied by XPS. As shown in Figure 6, the peaks corresponding to carbon, nitrogen, oxygen, silicon, and chlorine were clearly observed in the XPS elemental survey of the catalyst (Figure 6a). Deconvolution of the C 1s region showed peaks at 284.6 eV (C-C and C=C bonds),[78-81] 286.1 eV (C-N, C-O, and C-Cl bonds)[78-80] and 287.3 eV (C=O bond)[78,80] (Figure 6b). Figure 6c shows the nitrogen region of the XPS spectrum for piperazine-GO. It reveales the presence of a main peak at 399.1 eV related to tertiary amine[39,82] and two more peaks at 400.8 and 402.0 eV related to secondary amine[79] and N-H bonds,[82] respectively. As shown in Figure 6d, the peaks at 201.9 ($2P_{1/2}$) and 200.2 eV ($2P_{3/2}$), are assigned to the C-Cl bonds.[78,80] These peaks indicate that a small portion of chlorines remains unreacted. Furthermore, the higher resolution XPS signal for O atoms (Figure 6e) shows three peaks at 531.0, 532.3, and 533.8 eV that can be assigned to C=O, C-O and Si-O bonds.[81]

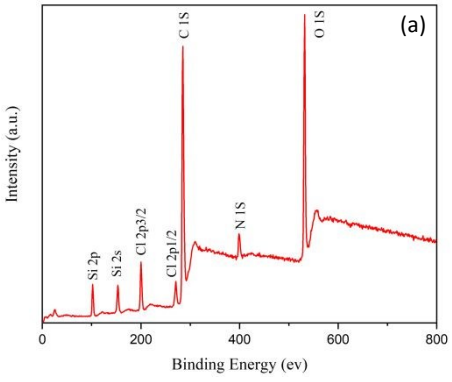

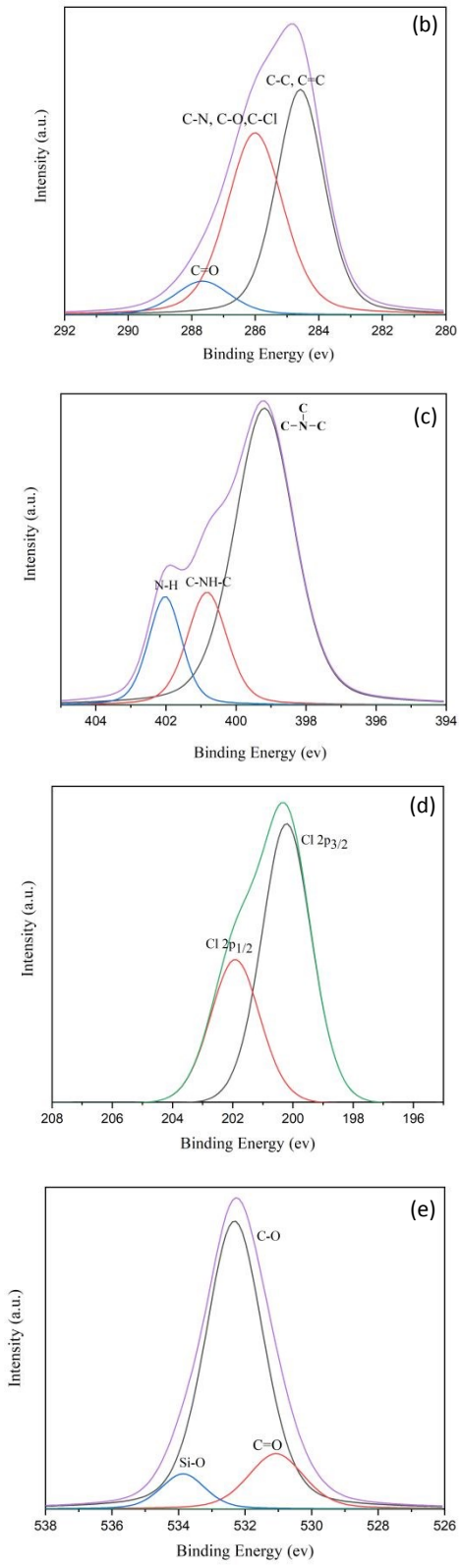

Figure 6. (a) XPS elemental survey spectrum, and high-resolution XPS spectra of (b) C 1s (c) N 1s (d) Cl 2p and (e) O 1s of the piperazine-GO.

Acid-base properties of the piperazine-GO were investigated through temperature-programmed desorption of ammonia (NH_3-TPD) and carbon dioxide (CO_2-TPD). In the NH_3-TPD profile of the catalyst (Figure 7a), the representative desorption peak at about 235-358 °C can be attributed to moderate Brønsted acidic sites. The CO_2-TPD profile of the catalyst revealed a desorption peak at 250-387 °C, which was assigned to moderate basic sites. The observed shoulder at 400-500 °C in the CO_2-TPD profile of the catalyst reflects the presence of strong Lewis basic sites. The desorption peak centered at about 543 °C in the NH_3-TPD and CO_2-TPD profiles was associated with the decomposition of the immobilized organic motifs on the support.[34] The contents of acidic and basic sites of the as-prepared catalyst were 2.76 and 2.94 mmol·g^{-1}, respectively. TPD analysis showed that the acidic and basic groups exist simultaneously in the piperazine-GO. Furthermore, the NH_3-TPD profile of the pristine GO (Figure 7a) revealed more acidic content (2.91 mmol·g^{-1}) in relatively lower temperature range (175-358 °C), compared with the piperazine-GO.[34]

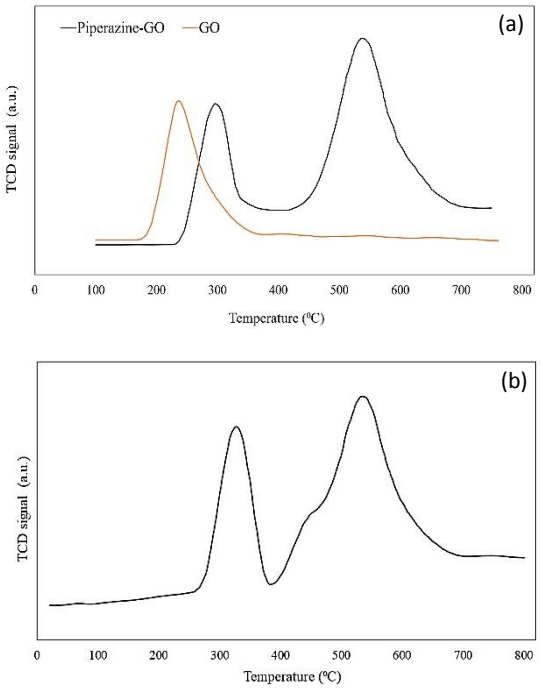

Figure 7. (a) NH_3-TPD profiles of piperazine-GO and GO; (b) CO_2-TPD profile of piperazine-GO.

Immobilization of piperazine on the water-dispersible GO (Figure 8a) altered the hydrophilic character of GO and made it a hydrophobic material in the aqueous media (Figure 8b-e).

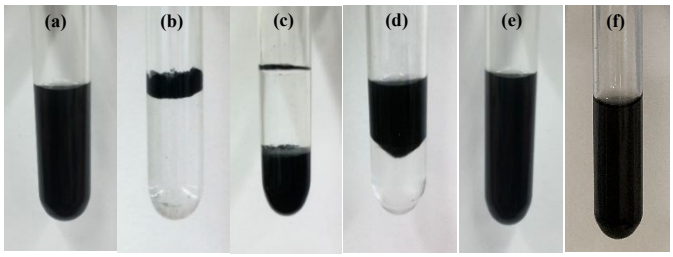

Figure 8. (a) GO in H_2O, (b) piperazine-GO in H_2O, (c) piperazine-GO in H_2O-$CHCl_3$, (d) piperazine-GO in H_2O-EtOAc, (e) piperazine-GO in H_2O-EtOH (1:1), (f) piperazine-GO in EtOH.

Catalytic performance of piperazine-GO for the synthesis of 2-amino-3-cyano-4*H*-chromenes

After full characterization of piperazine-GO, its catalytic activity was studied for the multicomponent synthesis of 2-amino-3-cyano-4*H*-chromenes. In this regard, the three-component reaction of 4-nitrobenzaldehyde (1 mmol), dimedone (1 mmol) and malononitrile (1 mmol) in the presence of piperazine-GO (1 mol%) at 50 °C as a test model was investigated for optimizing reaction parameters such as solvent, temperature and amount of the catalyst (Scheme 2, Table 1). The results of solvent screening revealed that they have a significant effect on the catalytic activity of piperazine-GO (Table 1, entries 1-9). The best result was obtained when the model reaction was conducted in EtOH:H_2O (1:1) (Table 1, entry 7). This reflects the higher solubility of the starting materials and also more dispersity of the catalyst in EtOH:H_2O (1:1) (Figure 8e). Moreover, the GO acidic functional groups could be well activated in aqueous solutions.[33,83] A similar reaction at lower temperatures proceeded over longer reaction times (Table 1, entries 10, 11). An increase in temperature did not have any effect on the progress of the reaction (Table 1, entry 12). When the model reaction was conducted in the presence of a lower amount of the catalyst, the same yield of the product was obtained within a longer reaction time (Table 1, entry 13). The significance of the catalyst in the reaction was demonstrated by conducting the reaction in the absence of the catalyst, which resulted in only a trace amount of the product (Table 1, entry 14). We have also prepared two catalysts from the reactions of 0.2 and 0.6 g of piperazine with 1 g of chloro-functionalized GO by the procedure given in the experimental section. The reaction of 4-nitrobenzaldehyde, dimedone and malononitrile was performed in the presence of these two catalysts and the results (Table 1, entries 15 and 16) were compared with that obtained in the presence of piperazine-GO. As shown in Table 1, piperazine-GO is the best choice for this reaction (entry 7), suggesting that 0.43 g of piperazine is the optimum amount for preparing the catalyst under the present conditions.

View Article Online DOI: 10.1039/D0GC01274B

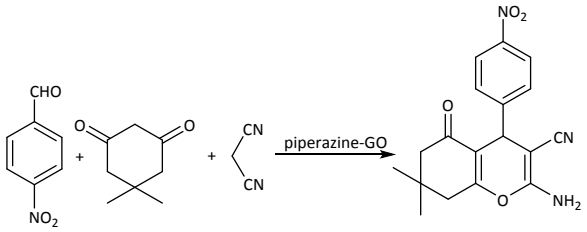

Scheme 2. One-pot three-component reaction of 4-nitrobenzaldehyde, dimedone and malononitrile catalyzed by piperazine-GO.

Table 1. One-pot three-component reaction of 4-nitrobenzaldehyde, dimedone and malononitrile catalyzed by piperazine-GO under different reaction conditions

Entry	Solvent	Catalyst (mol%)	T (°C)	Time (min)	Isolated Yield[a] (%)
1	H_2O	1	50	95	81
2	EtOH	1	50	50	90
3	EtOAc	1	50	80	75
4	$CHCl_3$	1	50	50	85
5	CH_3CN	1	50	90	65
6	Solvent-free	1	50	45	61
7	EtOH:H_2O (1:1)	1	50	10	90
8	EtOH:H_2O (1:2)	1	50	15	89
9	EtOH:H_2O (1:3)	1	50	30	82
10	EtOH:H_2O (1:1)	1	-	40	80
11	EtOH:H_2O (1:1)	1	40	30	90
12	EtOH:H_2O (1:1)	1	60	10	89
13	EtOH:H_2O (1:1)	0.5	50	20	90
14	EtOH:H_2O (1:1)	-	50	10	Trace
15	EtOH:H_2O (1:1)	1	50	60	45[b]
16	EtOH:H_2O (1:1)	1	50	10	90[c]

[a] Reaction conditions: 4-nitrobenzaldehyde (1 mmol), dimedone (1 mmol), malononitrile (1 mmol). The catalyst was prepared by using 0.43 g of piperazine and 1 g of chloro-functionalized GO as explained in the experimental section. [b] The catalyst was prepared by using 0.2 g of piperazine and 1 g of chloro-functionalized GO. [c] The catalyst was prepared by using 0.6 g of piperazine and 1 g of chloro-functionalized GO.

View Article Online
DOI: 10.1039/D0GC01274B

ARTICLE

Based on the optimized reaction conditions, we further extended the present method for the synthesis of various 2-amino-3-cyano-4*H*-chromene derivatives by using different types of aromatic/aliphatic aldehydes, dimedone and malononitrile (Scheme 3, Table 2). A number of aromatic aldehydes with electron-withdrawing/electron-donating groups underwent three-component reactions affording the desired products in high yields and short reaction times (Table 2, entries 1-15). The reactions of heterocyclic aldehydes, naphthaldehyde and cinnamaldehyde proceeded well (Table 2, entries 16-20). The applicability of this method was also examined for the condensation reaction of aliphatic aldehydes with dimedone and malononitrile. Fascinatingly, a variety of aliphatic aldehydes participated well in this reaction and the corresponding products were produced in good to high yields (Table 2, entries 21-28). This confirms the high versatility of the present catalytic system for the preparation of a wide range of biologically active 2-amino-3-cyano-4*H*-chromenes.

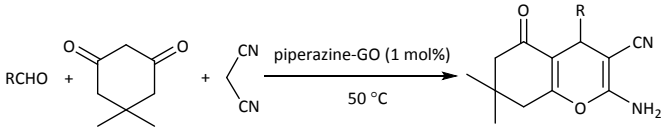

Scheme 3. One-pot three-component reaction of various aldehydes, dimedone and malononitrile catalyzed by piperazine-GO.

Table 2. One-pot three-component synthesis of various 2-amino-3-cyano-4*H*-chromenes catalyzed by piperazine-GO

Entry	R	Time (min)	Isolated Yield[a] (%)	M.P. (°C)	
				Obtained	Reported
1[84]	C_6H_5	15	95	230-232	231-233
2[84]	2-Cl-C_6H_4	5	98	189-192	188-191
3[84]	4-Cl-C_6H_4	20	98	206-208	206-209
4[85]	2,6-Cl_2-C_6H_3	10	98	236-238	236-238
5[86]	4-Br-C_6H_4	25	80	201-203	201-203
6[87]	2-O_2N-C_6H_4	5	94	223-225	223-226
7[84]	3- O_2N-C_6H_4	5	91	209-211	208-210
8[86]	4-O_2N-C_6H_4	10	90	172-174	171-172
9[84]	4-NC-C_6H_4	10	95	213-215	212-213
10[88]	4-Me-C_6H_4	45	82	209-211	208-210
11[86]	4-MeO-C_6H_4	45	80	187-189	186-188
12[85]	2,4-$(MeO)_2$-C_6H_4	25	81	181-183	180-182
13[84]	3,4-$(MeO)_2$-C_6H_4	30	90	176-179	175-178
14[84]	3,4,5-$(MeO)_3$-C_6H_2	15	89	177-179	175-179
15[89]	4-MeCONH-C_6H_4	30	95	247-249	247-248
16[84]	2-Thienyl	45	86	222-224	223-227
17[84]	2-Furyl	25	96	194-197	195-197
18[87]	3-Pyridyl	10	95	249-251	250-252
19[90]	1-Naphthyl	30	86	243-246	243-245
20[86]	C_6H_5CH=CH	30	85	183-185	182-184

View Article Online
DOI: 10.1039/D0GC01274B

21[91]	H	30	89	189-191	190-192
22[91]	Me	30	92	181-184	180-183
23	Me_2CH	90	80	199-201	-
24	Me_2CHCH_2	45	84	196-200	-
25[86]	$CH_3(CH_2)_2$	60	80[b]	173-175	172-174
26[86]	$CH_3(CH_2)_3$	90	72[b]	164-166	165-167
27[87]	$CH_3(CH_2)_5$	150	80[b]	185-187	187-189
28[92]	$CH_3(CH_2)_6$	150	73[b]	157-159	156-158

[a] Reaction conditions: aldehyde (1 mmol), dimedone (1 mmol), malononitrile (1 mmol), piperazine-GO (1 mol%), 50˚C, H_2O-EtOH (1:1, 1 mL, except for entries 25-28); [b] Refluxing EtOH (2 mL).

Furthermore, the reaction was extended to activated compounds such as cyclohexane-1,3-dione, acetylacetone and methylacetoacetate containing enolizable C–H bonds, 2-naphthol and 4-hydroxycoumarin (Scheme 4). The products were obtained in high yields and in reasonable reaction times by replacing dimedone with these activated compounds.

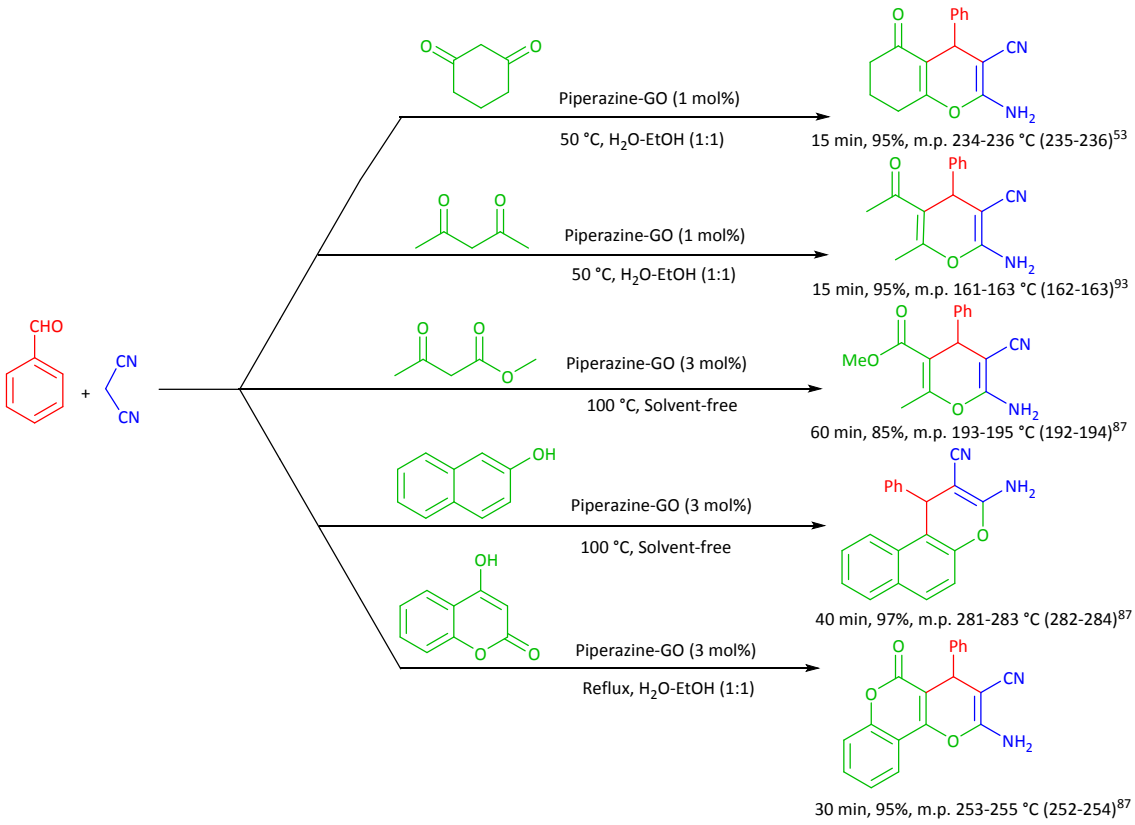

Scheme 4. One-pot three-component reaction of benzaldehyde, malononitrile and activated compounds containing enolizable C–H bonds, 2-naphthol and 4-hydroxycoumarin.

The recovery and reuse of the catalysts are highly preferable in terms of green synthetic processes. Consequently, the reusability of piperazine-GO was investigated for the model reaction under the optimized reaction conditions. After completion of the reaction, which was monitored by TLC, the reaction mixture was cooled to room temperature and the catalyst was separated by simple centrifugation, washed with EtOH to remove organic products, and then dried and reused. The recyclability test was stopped after six runs and it was found that the reduction in the activity and the amount of the catalyst (2.5%) after six times reuse is negligible (Figure 9). Comparison of the FT-IR, $^{29}Si\{^1H\}$ and $^{13}C\{^1H\}$ CP/MAS NMR spectra and TEM image of the used catalyst (Figures 10-12) with those of the fresh catalyst shows that the structure and morphology of piperazine-GO remain intact after six times reuse.

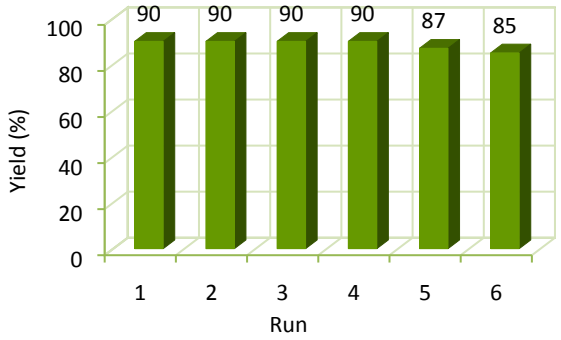

Figure 9. Reusability of the piperazine-GO in the one-pot three-component reaction of 4-nitrobenzaldehyde, malononitrile and dimedone under optimized reaction conditions, in 10 min.

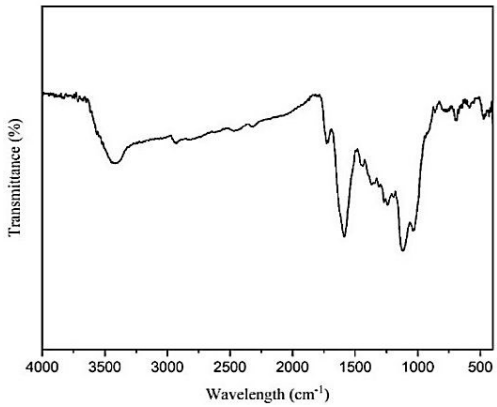

Figure 10. FT-IR spectrum of piperazine-GO after six times reuse.

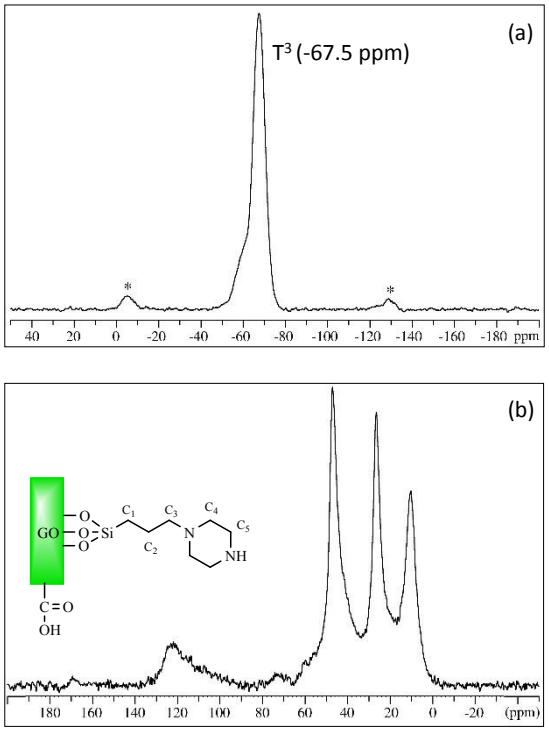

Figure 11. (a) $^{29}Si\{^{1}H\}$ CP/MAS NMR (9.39 T) and (b) $^{13}C\{^{1}H\}$ CP/MAS NMR (9.39 T) spectra of piperazine-GO after six times reuse, acquired with a CP contact time of 1.0 ms and spinning speeds of 5.0 kHz and 10.0 kHz, respectively. The asterisks indicate spinning sidebands.

View Article Online
DOI: 10.1039/D0GC01274D

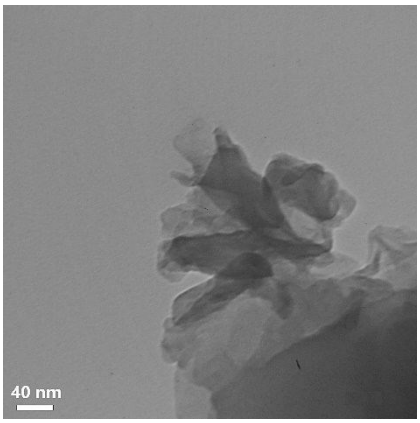

Figure 12. TEM image of piperazine-GO after six times reuse.

Furthermore, the XPS analysis of the recycled piperazine-GO after six runs confirmed the preservation of the electronic features for all elements (Figure 13). These findings strongly suggest the suitable stability and durability of the catalyst.

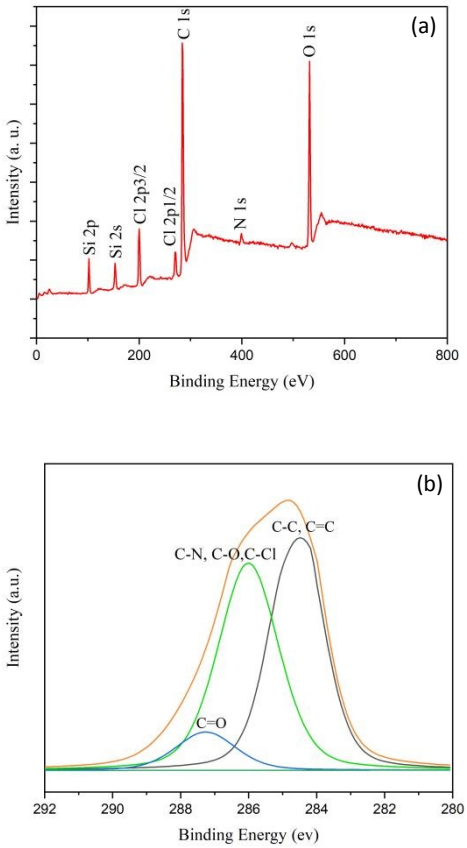

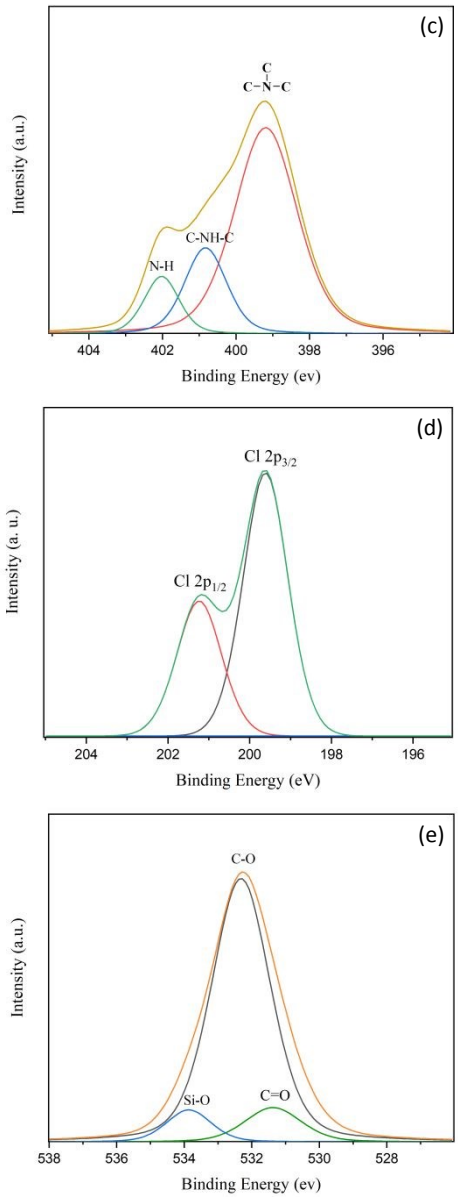

Figure 13. (a) XPS elemental survey spectrum, and high-resolution XPS spectra of (b) C 1s (c) N 1s (d) Cl 2p and (e) O 1s of the piperazine-GO after six times reuse.

To test the potential synthetic applications of this method, a larger scale reaction of 4-nitrobenzaldehyde (50 mmol), dimedone (50 mmol) and malononitrile (50 mmol) was carried out under the present reaction conditions. The reaction proceeded in 10 min, giving 90% yield of the desired product.

In order to find the role of the catalyst, one-pot three-component reaction of 4-nitrobenzaldehyde, dimedone, and malononitrile in the presence of GO, piperazine and a physical mixture of GO + piperazine were examined under the optimized reaction conditions (Figure 14). The highest yield of the desired product was produced in the presence of piperazine-GO. The reaction of 4-nitrobenzaldehyde and malononitrile, which produces the Knoevenogel product and the reaction of the Knoevenogel product with dimedone (two-pot synthesis of 2-amino-3-cyano-4*H*-chromene) in the presence of GO, piperazine and a physical mixture of GO + piperazine were also investigated. Piperazine-GO exhibited higher catalytic activity than GO, piperazine and a physical mixture of GO + piperazine in the formation of the Knoevenogel product and also in the two-pot synthesis of 2-amino-3-cyano-4*H*-chromene, due to the synergetic effect of piperazine as a basic group and inherent carboxylic acids on the GO. These results revealed that the three-component reaction of dimedone, malononitrile and 4-nitrobenzaldehyde is catalyzed by piperazine and also by carboxylic acids on the GO.

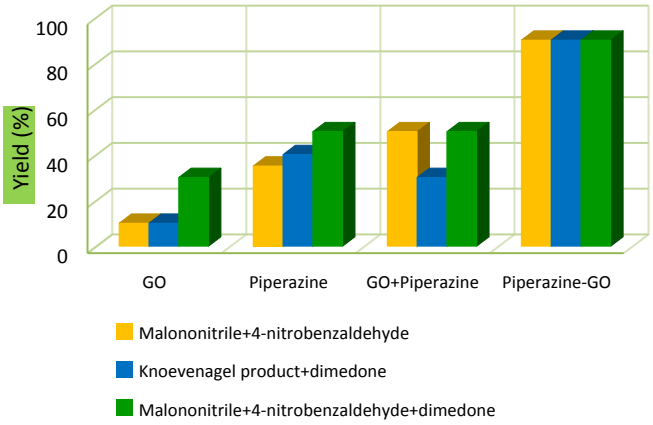

Figure 14. Effect of various active groups such as GO, piperazine, GO + piperazine and piperazine-GO on the synthesis of the Knoevenogel product and one-pot three-component and also the two-pot synthesis of 2-amino-3-cyano-4*H*-chromene after 10 min.

Based on these observations, a mechanism which is supported by the literature[66,87,89] for the multicomponent synthesis of 2-amino-3-cyano-4*H*-chromene is outlined in Scheme 5. The process represents a typical tandem reaction by multiple-activation. At first, the acid sites present in the catalyst, activate the carbonyl groups in the aldehyde to react with activated malononitrile by piperazine as a basic functional group to form the Knoevenagel product (Figure S23) upon dehydration. Michael-type addition reaction of the enol form of dimedone with the Knoevenagel product, followed by intramolecular nucleophilic cyclization, produces the desired product (see the reaction time curve in Figure S24).

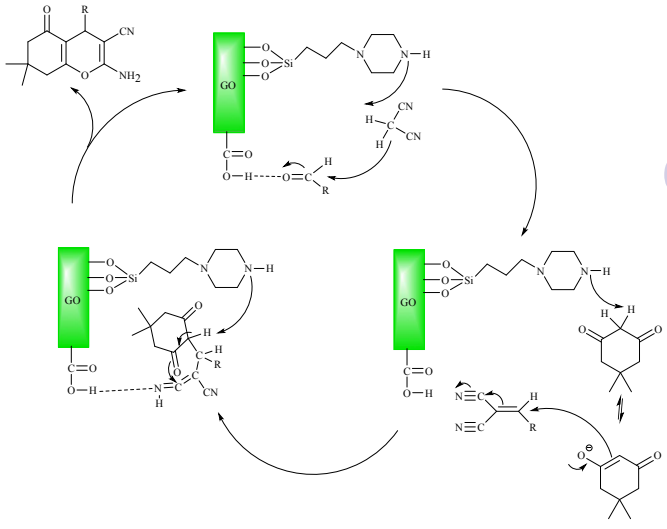

Scheme 5. A plausible mechanism for the one-pot three-component reaction of aldehyde, dimedone and malononitrile in the presence of piperazine-GO.

To show the merits of the present method for the synthesis of 2-amino-3-cyano-4*H*-chromenes, we have compared the catalytic activity of piperazine-GO with various basic, acidic and bifunctional catalysts reported for the one-pot three-component reaction of aldehydes, dimedone and malononitrile (Table 3). From Table 3, it appears that piperazine-GO provides significant advantages in terms of turnover number (TON) compared with the other catalytic systems. It is worth to note that most of the reported methods suffer from a lack of generality for the synthesis of 2-amino-3-cyano-4*H*-chromenes from aliphatic aldehydes. 2-Amino-3-cyano-4*H*-chromene containing aliphatic aldehydes could be efficiently synthesized by our catalytic method. These promising results should be attributed to the synergistic cooperative effect of both acidic and basic groups in the piperazine-GO. Moreover, due to the homogeneous distribution of the active sites along with the crumpling structure of the catalyst, reactants and products can easily access or leave the active sites on both sides of the two-dimensional catalyst with negligible mass transfer resistance. Importantly, some of the reported methods proceed *via* a two-pot procedure (entries 5, 6 and 9). These methods were used for the asymmetric synthesis of 2-amino-3-cyano-4*H*-chromenes. Clearly, the catalyst separation is troublesome in the case of the homogeneous catalysts.

Table 3. Comparison of the catalytic activity of piperazine-GO with some basic, acidic and bifunctional catalysts reported for the one-pot three-component reaction of aldehydes, dimedone and malononitrile

Entry	Catalyst (mol%)	Reaction conditions	Aldehyde	Time (min)	Yield (%)	TON[a]
1[87]	Piperazine (11)	H_2O, 90 °C	Aryl	4-28	91-98	8.2-8.9
2[87]	Piperazine (33)	H_2O, r.t.	Aryl	35-170	90-97	2.7-2.9
3[61]	$CaCl_2$ (20)	EtOH, r.t.	Aryl	35-120	89-96	4.4-4.8
4[61]	$CaCl_2$ (20)	EtOH, Ultrasound	Aryl	5-15	91-97	4.5-4.8
5[62]	Asymmetric organocatalyst[b,c] (2)	Et_2O, r.t.	Aryl	4 h	83	41.5
6[63]	Squaramides[b] (5)	THF, 4 °A MS, 0 °C	Aryl	5 h	94-99	18.8-19.8
7[64]	sodium alginate (10)	EtOH, Reflux	Aryl	34-150	80-96	8-9.6
8[67]	Ce-V/SiO_2 (4.28)	EtOH, r.t.	Aryl	60	87-95	20.3-22.2
9[68]	Asymmetric organocatalyst[b,d] (20)	Silica gel (30 mg), THF, r.t.	Aryl	8-16 h	85-96	4.2-4.8
10[94]	Piperazine (15)	Solvent-free, Ball-milling, r.t.	Aryl	20-120	88-96	5.8-6.4
11[95]	MCM-41-NH_2 (10)	H_2O, 70 °C	Aryl/Alkyl	0.5-7 h	45-95	4.5-9.5
12[96]	MOF[e]–NH_2 (6)	EtOH, Reflux	Aryl	4 h	80-96	13.3-16
13[97]	Urea (10)	H_2O-EtOH (1:1), r.t.	Aryl/Alkyl	2-16 h	80-96	8-9.6
14[98]	[Ch][Tau][f] IL (5)	H_2O-EtOH (1:1), Reflux	Aryl	2-3 h	78-94	15.6-18.8
15[92]	[bmIm]OH IL (20)	Solvent-free, r.t.	Aryl	5-20	85-98	4.2-4.9
16[99]	MNP-DMAP[g] (5)	H_2O, 80 °C	Aryl	0.5-5 h	90-98	18-19.6
17[54]	$[DiEG(mim)_2][OH]_2$[h] (10)	H_2O, K_2CO_3 (10 mol%), r.t.	Aryl	15-45	85-92	8.5-9.2
18[100]	$H_5BW_{12}O_{40}$ (10)	EtOH-H_2O (1:1), Reflux	Aryl	1-5 h	85-98	8.5-9.8
19[101]	VSA NRs[i] (5)	H_2O-EtOH, Reflux	Aryl	5-50	78-98	15.6-19.6
20	Piperazine-GO (1)	H_2O-EtOH (1:1), 50 °C	Aryl/Alkyl	5-150	70-98	70-98

[a] TON = mmol of the product per mmol of the catalyst; [b] The reactions proceed *via* a two-step method; [c] 1-(((1*R*, 4a*S*, 10a*R*)-7-*Iso*-propyl-1, 4a-dimethyl l-1,2,3,4,4a,9,10,10a-octahydrophenanthren-1-yl) methyl)-3-((1*R*)-(6-methoxyquinolin-4-yl)(8-vinylquinuclidin-2-yl)-methyl)thiourea; [d] (*S*)-2-amino-*N*-[(1*R*,2*R*)-2-(4-methylphenylsulfonamido) cyclohexyl] aryl/sulphonamide; [e] Metal–organic framework; [f] Choline taurinate; [g] 4-(Dimethylamino)pyridine; [h] Diethylene glycol-bis(3-methylimidazolium) dihydroxide; [i] Nanorod vanadate sulfuric acid

Finally, a series of green metrics[102,103] such as atom economy (AE), atom efficiency (AE_f), carbon efficiency (CE), reaction mass efficiency (RME), optimum efficiency (OE), process mass intensity (PMI), E-factor (E), solvent intensity (SI), and water intensity (WI) were calculated to evaluate the greenness of the one-pot three-component reaction of aldehydes, dimedone and malononitrile (Figure 15, see ESI for detailed calculations). As it is shown in Figure 15a, the high values of the AE, AE_f, CE, RME and OE for the synthesis

of three 2-amino-3-cyano-4*H*-chromene derivatives of Table 2 (entries 1, 3 and 8), indicate well the greenness of the process. The lower the PMI, E and SI, the more desirable is the process in view of green chemistry. These values are less than 50 in the synthesis of the above-mentioned 2-amino-3-cyano-4*H*-chromenes (Figure 15b). Very small amounts of WI were also obtained in these processes (Figure 15b). The organic solvent, which was used in these protocols was EtOH. Therefore, it can be concluded that regarding the high values of RME and low values of PMI, E, SI and WI, this one-pot three-component process is an efficient and green protocol for the synthesis of 2-amino-3-cyano-4*H*-chromenes.

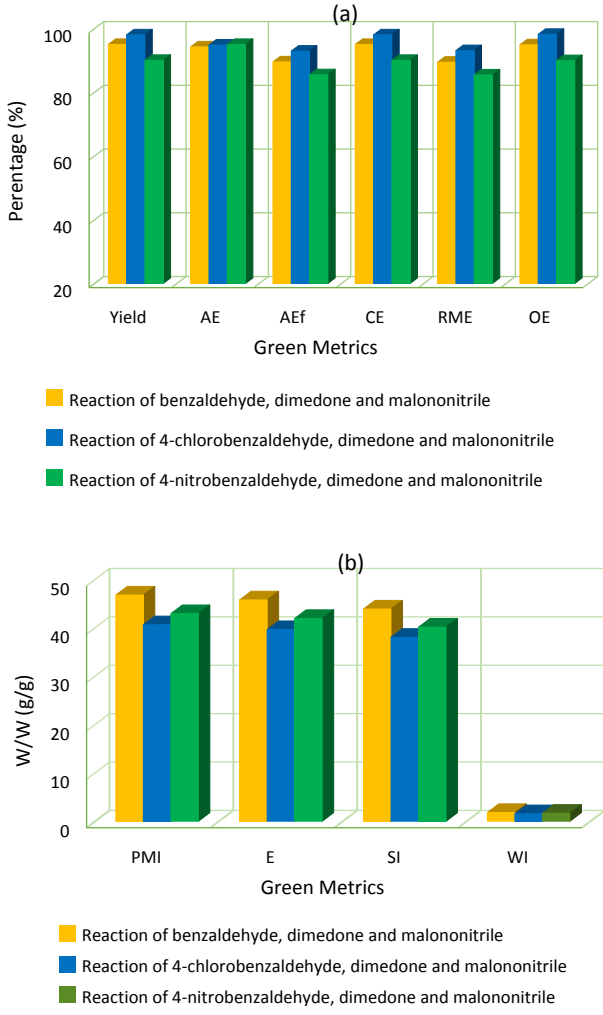

Figure 15. Green metrics including (a) AE, AE_f, CE, RME, OE and (b) PMI, E, SI, and WI for the one-pot three-component reactions of aldehyde (benzaldehyde/4-chlorobenzaldehyde/4-nitrobenzaldehyde), dimedone and malononitrile (entries 1, 3 and 8 in Table 2); W/W = Weight/Weight (g/g)

To prove the more greenness of the current catalyst over the reported catalysts in the one-pot three-component reaction of benzaldehyde, dimedone and malononitrile, the green metrics of the current catalyst were compared with those of two previously reported catalysts[54,67] (Table 3, entries 8 and 17). As can be perceived from the results in Figure 16a and b, the higher the AE_f, CE and RME factors and the lower the PMI, E, SI and WI factors of piperazine-GO compared with those of Ce-V/SiO_2 and [DiEG(mim)$_2$][OH]$_2$, confirmed that the piperazine-GO is a greener and more sustainable catalyst for such a MCR (see ESI for detailed calculations).

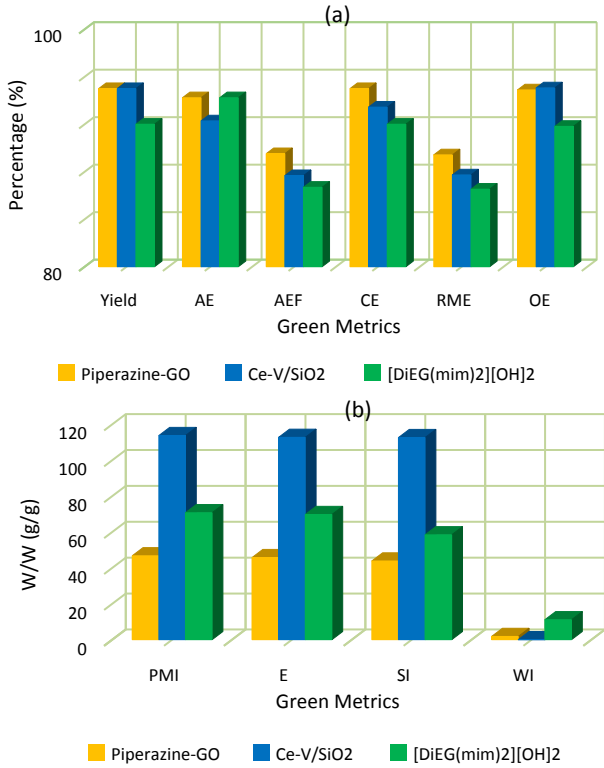

Figure 16. Green metrics including (a) AE, AE_f, CE, RME, OE and (b) PMI, E, SI and WI for the one-pot three-component reaction of benzaldehyde, dimedone and malononitrile catalyzed by piperazine-GO (this study), Ce-V/SiO_2 (Table 3, entry 8) and [DiEG(mim)$_2$][OH]$_2$ (Table 3, entry 17); W/W = Weight/Weight (g/g)

Conclusions

In summary, a new inexpensive and reusable bifunctional acid-base catalyst obtained by post grafting of piperazine onto GO (piperazine-GO) was synthesized and characterized by different methods such as FT-IR, solid-state $^{29}Si\{^1H\}$ and $^{13}C\{^1H\}$ CP/MAS NMR, elemental analysis, TGA, TEM, FE-SEM, XPS and TPD. The catalyst was successfully used as a bifunctional acid-base catalyst for the one-pot three-component synthesis of 2-amino-3-cyano-4*H*-chromenes. A wide range of 2-amino-3-cyano-4*H*-chromenes was synthesized from the reaction of malononitrile, various aryl/alkyl aldehydes and active compounds containing enolizable C–H bonds in aqueous ethanol. The promising results should be attributed to the synergetic cooperative effects of both acidic and basic groups in piperazine-GO. This approach offers several advantages such as good to high yields of the products, short reaction times, the use of a simplified one-pot synthetic process and green reaction media, step saving, the least amount of waste, scalability, low operational cost and facile catalyst recovery and reuse. Furthermore, the series of green metrics analysis

for the reaction processes has been performed, which provided favorable results for the present approach.

Conflicts of interest

There are no conflicts to declare.

Acknowledgments

Financial support of this project by the University of Birjand Research Council and access to the solid-state NMR facilities at the Department of Chemistry, Aarhus University and the XPS facilities of the University of Alicante are acknowledged.

References

1 O. Jiménez, G. de la Rosa and R. Lavilla, *Angew. Chem., Int. Ed.,* 2005, **44**, 6521-6525.
2 R. Y. Guo, Z. M. An, L. P. Mo, R. Z. Wang, H. X. Liu, S. X. Wang and Z. H. Zhang, *ACS Comb. Sci.,* 2013*,* **15***,* 557-563*.*
3 A. Maleki, *Tetrahedron,* 2012*,* **68***,* 7827-7833*.*
4 M. Kanai, N. Kato, E. Ichikawa and M. Shibasaki, *Pure Appl. Chem.,* 2005*,* **77***,* 2047-2052.
5 Y. Shen, X. Feng, Y. Li, G. Zhang and Y. Jiang, *Tetrahedron,* 2003*,* **59**, 5667-5675.
6 S. Kanemasa and K. Ito, *Eur. J. Org. Chem.,* 2004*,* **23***,* 4741-4753.
7 J. A. Ma and D. Cahard, *Angew. Chem., Int. Ed.,* 2004, **43**, 4566-4583.
8 Y. Wang, H. Li, Y. Q. Wang, Y. Liu, B. M. Foxman and L. Deng, *J. Am. Chem. Soc.,* 2007, **129***,* 6364-6365.
9 Y. M. Lin, J. Boucau, Z. Li, V. Casarotto, J. Lin, A. N. Nguyen and J. Ehrmantraut, *Org. Lett.,* 2007*,* **9***,* 567-570.
10 S. B. Tsogoeva, M. J. Hateley, D. A. Yalalov, K. Meindl, C. Weckbecker and K. Huthmacher, *Bioorg. Med. Chem.,* 2005, **13**, 5680-5685.
11 S. F. Mayer, W. Kroutil and K. Faber, *Chem. Soc. Rev.*, 2001, **30**, 332-339.
12 D. E. Cane, *Chem. Rev*., 1990, **90**, 1089-1103.
13 O. Pamies and J. E. Bäckvall, *Chem. Rev*., 2003, **103**, 3247-3261.
14 S. Shylesh and W. R. Thiel, *ChemCatChem*, 2011, **3**, 278-287.
15 K. Motokura, M. Tomita, M. Tada and Y. Iwasawa, *Chem. Eur. J.,* 2008, **14**, 4017-4027.
16 E. L. Margelefsky, R. K. Zeidan and M. E. Davis, *Chem. Soc. Rev.*, 2008, **37**, 1118-1126.
17 N. A. Brunelli, K. Venkatasubbaiah and C. W. Jones, *Chem. Mater.,* 2012, **24**, 2433-2442.
18 D. Bahulayan, L. John and M. Lalithambika, *Synth. Commun*., 2003, **33**, 863-869.
19 K. Motokura, M. Tada and Y. Iwasawa, *Chem. Asian J.,* 2008, **3**, 1230-1236.
20 W. Yu, Y. Tang, L. Mo, P. Chen, H. Lou and X. Zheng, *Catal. Commun*., 2011, **13**, 35-39.
21 R. K. Zeidan, S. J. Hwang and M. E. Davis, *Angew. Chem., Int. Ed.,* 2006, **45**, 6332-6335.
22 C. Wang, F. Shang, X. Yu, J. Guan and Q. Kan, *Appl. Surface Sci.*, 2012, **258**, 6846-6852.
23 F. Shang, J. Sun, S. Wu, Y. Yang, Q. Kan and J. Guan, *Micropor. Mesopor. Mat.*, 2010, **134**, 44-50.
24 L. Deiana, Y. Jiang, C. Palo-Nieto, S. Afewerki, C. A. Incerti-Pradillos, O. Verho and A. Córdova, *Angew. Chem., Int. Ed.,* 2014, **53**, 3447-3451.
25 F. X. Felpin and E. Fouquet, *ChemSusChem*, 2008, **1**, 718-724.
26 K. Motokura, M. Tada and Y. Iwasawa, *J. Am. Chem. Soc.,* 2007, **129**, 9540-9541.
27 Y. Yang, X. Liu, X. Li, J. Zhao, S. Bai, J. Liu and Q. Yang, *Angew. Chem., Int. Ed.,* 2012, **51**, 9164-9168.
28 S. Shylesh, A. Wagener, A. Seifert, S. Ernst and W. R. Thiel, *Angew. Chem., Int. Ed*., 2010, **49**, 184-187.
29 Y. Huang, S. Xu and V. S. Y. Lin, *Angew. Chem., Int. Ed*., 2011, **50**, 661-664.
30 J. Pyun, *Angew. Chem., Int. Ed.,* 2011, **50**, 46-48.
31 Y. Zhu, S. Murali, W. Cai, X. Li, J. W. Suk, J. R. Potts and R. S. Ruoff, *Adv. Mater.,* 2010, **22**, 3906-3924.
32 S. Kundu and B. Basu, *RSC Adv*., 2015, **5**, 50178-50185.
33 O. Mohammadi, M. Golestanzadeh and M. Abdouss, *New J. Chem.,* 2017, **41***,* 11471-11497.
34 F. Zhang, H. Jiang, X. Li, X. Wu and H. Li, *ACS Catal*., 2013, **4**, 394-401.
35 H. R. E. Zand, H. Ghafuri and N. Ghanbari, *ChemistrySelect*, 2018, **3**, 8229-8237.
36 B. Dam, R. Jamatia, A. Gupta and A. K. Pal, *ACS Sustain. Chem. Eng.,* 2017, **5**, 11459-11469.
37 B. Xue, J. Zhu, N. Liu and Y. Li, *Catal. Commun*., 2015, **64**, 105-109.
38 Y. Li, Q. Zhao, J. Ji, G. Zhang, F. Zhang and X. Fan, *RSC Adv*., 2013, **3**, 13655-13658.
39 W. Zhang, Q. Zhao, T. Liu, Y. Gao, Y. Li, G. Zhang, F. Zhang and X. Fan, *Ind. Eng. Chem. Res.*, 2014, **53**, 1437-1441.
40 W. Zhang, H. Gu, Z. Li, Y. Zhu, Y. Li, G. Zhang, F. Zhang and X. Fan, *J. Mater. Chem. A,* 2014, **2**, 10239-10243.
41 S. Sobhani and F. Zarifi, *RSC Adv.,* 2015, **5**, 96532-96538.
42 S. Sobhani, F. Zarifi and J. Skibsted, *ChemistrySelect*, 2016, **1**, 2945-2951.
43 S. Sobhani, F. Zarifi and J. Skibsted, *New J. Chem.*, 2017, **41**, 6219-6225.
44 S. Sobhani, F. Zarifi, F. Barani and J. Skibsted, *Org. Chem. Res.,* 2019, **5**, 117-127.
45 S. Sobhani, F. Zarifi and J. Skibsted, *ACS Sustain. Chem. Eng.,* 2017, **5***,* 4598-4606.
46 A. Sengupta, C. Su, C. Bao, C. T. Nai and K. P. Loh, *ChemCatChem*, 2014, **6***,* 2507-2511.
47 A. M. El-Saghier, M. B. Naili, B. K. Rammash, N. A. Saleh and K. M. Kreddan, *ARKIVOC*, 2007, **16**, 83-91.

48 R. R. Kumar, S. Perumal, P. Senthilkumar, P. Yogeeswari and D. Sriram, *Bioorg. Med. Chem. Lett.,* 2007, **17**, 6459-6462.
49 M. Kidwai, R. Poddar, S. Bhardwaj, S. Singh and P. M. Luthra, *Eur. J. Med. Chem.,* 2010, **45**, 5031-5038.
50 D. Kumar, V. B. Reddy, S. Sharad, U. Dube and S. Kapur, *Eur. J. Med. Chem.,* 2009, **44**, 3805-3809.
51 A. Tanabe, H. Nakashima, O. Yoshida, N. Yamamoto, O. Tenmyo and T. Oki, *J. Antibiotics*, 1988, **41**, 1708-1710.
52 A. Bolognese, G. Correale, M. Manfra, A. Lavecchia, O. Mazzoni, E. Novellino and R. Loddo, *J. Med. Chem*., 2004, **47**, 849-858.
53 O. Rosati, A. Pelosi, A. Temperini, V. Pace and M. Curini, *Synthesis*, 2016, **48**, 1533-1540.
54 K. Niknam, M. Khataminejad and F. Zeyaei, *Tetrahedron Lett.,* 2016, **57**, 361-365.
55 A. Molla and S. Hussain, *RSC Adv.,* 2016, **6**, 5491-5502.
56 D. Azarifar, S. M. Khatami and R. Nejat-Yami, *J. Chem. Sci.,* 2014, **126**, 95-101.
57 K. S. Pandit, P. V. Chavan, U. V. Desai, M. A. Kulkarni and P. P. Wadgaonkar, *New J. Chem.,* 2015, **39**, 4452-4463.
58 H. Kiyani and F. Ghorbani, *Res. Chem. Inter*., 2015, **41**, 7847-7882.
59 M. Norouzi, D. Elhamifar, R. Mirbagheri and Z. Ramazani, *J. Taiwan Inst. Chem. Eng.*, 2018, **89**, 234-244.
60 S. Sadjadi, M. M. Heravi, V. Zadsirjan and V. Farzaneh, *Appl. Surface Sci.*, 2017, **426**, 881-889.
61 H. R. Safaei, M. Shekouhy, A. Shirinfeshan and S. Rahmanpur, *Mol. Divers.*, 2012, **16**, 669-683.
62 G. Zhang, Y. Zhang, J. Yan, R. Chen, S. Wang, Y. Ma and R. Wang, *J. Org. Chem.,* 2012, **77**, 878-888.
63 Y. Gao and D. M. Du, *Tetrahedron Asymmetry*, 2012, **23**, 1343-1349.
64 M. G. Dekamin, S. Z. Peyman, Z. Karimi, S. Javanshir, M. R. Naimi-Jamal and M. Barikani, *Inter. J. Biol. Macromol.*, 2016, **87**, 172-179.
65 M. Norouzi and D. Elhamifar, *Catal. Lett*., 2019, **149**, 619-628.
66 A. Yaghoubi and M. G. Dekamin, *ChemistrySelect*, 2017, **2**, 9236-9243.
67 S. N. Maddila, S. Maddila, W. E. van Zyl and S. B. Jonnalagadda, *Chem. Open*, 2016, **5**, 38-42.
68 R. L. Magar, P. B. Thorat, B. R. Patil and R. P. Pawar, *Current Organocatal*., 2018, **5**, 74-81.
69 S. Sobhani, F. O. Chahkamali and J. M. Sansano, *RSC Adv.,* 2019, **9**, 1362-1372.
70 S. Sobhani, Z. 67M. Falatooni and M. Honarmand, *RSC Adv.*, 2014, **4**, 15797-15806.
71 S. Sobhani, H. Hosseini Moghadam, J. Skibsted and J. M. Sansano, *Green Chem*., 2020, **22**, 1353-1365.
72 S. Sobhani and R. Jahanshahi, *New J. Chem*., 2013, **37**, 1009-1015.
73 S. Sobhani and Z. Ramezani, *RSC Adv.,* 2016, **6**, 29237-29244.
74 S. Sobhani and Z. Zeraatkar, *Appl. Organomet. Chem.,* 2016, **30**, 12-19.
75 W. Wu, Y. Xu, H. Wu, J. Chen, M. Li, T. Chen, J. Hong and L. Dai, *J. Appl. Polym. Sci.*, 2020, **137**, 47710.
76 L. Zhang, H. Wu, M. Wei, Z. Zheng, D. D. Vu, T. T. X. Bui and X. Huang, *J. Coat. Technol. Res.*, 2018, **15**, 1343-1356.
77 V. H. Pham, H. D. Pham, T. T. Dang, S. H. Hur, E. J. Kim, B. S. Kong, S. Kim and J. S. Chung, *J. Mater. Chem.*, 2012, **22**, 10530-10536.
78 D. Bouša, J. Luxa, V. Mazanek, O. Jankovský, D. Sedmidubský, K. Klímová and Z. Sofer, *RSC Adv*., 2016, **6**, 66884-66892.
79 M. Frey, R. K. Zenn, S. Warneke, K. Müller, A. Hintennach, R. E. Dinnebier and M. R. Buchmeiser, *ACS Energy Lett.*, 2017, **2**, 595-604.
80 J. Zheng, H. T. Liu, B. Wu, C. A. Di, Y. L. Guo, T. Wu and D. B. Zhu, *Sci. Rep.*, 2012, **2**, 662.
81 M. K. Rabchinskii, A. T. Dideikin, D. A. Kirilenko, M. V. Baidakova, V. V. Shnitov, F. Roth and N. M. Lebedeva, *Sci. Rep.*, 2018, **8**, 14154.
82 W. Zhang, S. Wang, J. Ji, Y. Li, G. Zhang, F. Zhang and X. Fan, *Nanoscale*, 2013, **5**, 6030-6033.
83 A. M. Dimiev, L. B. Alemany and J. M. Tour, *ACS nano*, 2013, **7**, 576-588.
84 Y. Wan, W. W. Liu, Q. C. Zhan, H. Cui, Q. Zhang, S. N. Yue and H. Wu, *Lett. Org. Chem*., 2015, **12**, 538-543.
85 N. M. Abd El-Rahman, A. A. El-Kateb and M. F. Mady, *Synth. Commun.*, 2007, **37**, 3961-3970.
86 L. M. Wang, J. H. Shao, H. Tian, Y. H. Wang and B. Liu, *J. Fluorine Chem.,* 2006, **127**, 97-100.
87 M. R. Yousefi, O. Goli-Jolodar and F. Shirini, *Bioorg. Chem.*, 2018, **81**, 326-333.
88 M. Hong and C. Cai, *J. Chem. Res.*, 2010, **34**, 568-570.
89 S. Balalaie, M. Sheikh-Ahmadi and M. Bararjanian, *Catal. Commun*., 2007, **8**, 1724-1728.
90 V. Bhaskar, R. Chowdary, S. R. Dixit and S. D. Joshi, *Bioorg. Chem.,* 2019, **84**, 202-210.
91 B. Paplal, S. Nagaraju, P. Veerabhadraiah, K. Sujatha, S. Kanvah, B. V. Kumar and D. Kashinath, *RSC Adv*., 2014, **4**, 54168-54174.
92 B. C. Ranu, S. Banerjee and S. Roy, *Indian J. Chem*., 2008, **47B**, 1108-1112.
93 F. Tamaddon and D. Azadi, *J. Iran. Chem. Soc.,* 2017, **14**, 2077-2086.
94 M. Amirnejad, M. R. Naimi-Jamal, H. Tourani and H. Ghafuri, *Monatsh. Chem*., 2013, **144**, 1219-1225.
95 M. Mirza-Aghayan, S. Nazmdeh, R. Boukherroub, M. Rahimifard, A. A. Tarlani and M. Abolghasemi-Malakshah, *Synth. Commun*., 2013, **43**, 1499-1507.
96 V. Safarifard, S. Beheshti and A. Morsali, *CrystEngComm*, 2015, **17**, 1680-1685.
97 G. Brahmachari and B. Banerjee, *ACS Sustain. Chem. Eng.,* 2014, **2**, 411-422.
98 W. Deng, L. Liu and Y. Peng, *Green Process Synth.,* 2018, **7**, 191-197.
99 S. K. Dangolani, F. Panahi, M. Nourisefat and A. Khalafi-Nezhad, *RSC Adv*., 2016, **6**, 92316-92324.

View Article Online
DOI: 10.1039/D0GC01274B

100 M. M. Heravi, M. Mirzaei, S. Y. S. Beheshtiha, V. Zadsirjan, F. Mashayekh Ameli and M. Bazargan, *Appl. Organomet. Chem.,* 2018, **32**, e4479.
101 M. Nasr-Esfahani and T. Abdizadeh, *J. Nanosci. Nanotechnol*., 2013, **13**, 5004-5011.
102 F. Roschangar, R. A. Sheldon and C. H. Senanayake, *Green Chem.*, 2015, **17**, 752-768.
103 D. J. Constable, A. D. Curzons and V. L. Cunningham, *Green Chem.*, 2002, **4**, 521-527.